ACS EARTH AND SPACE CHEMISTRY

http://pubs.acs.org/journal/aesccq

Article

Nitrous Acid (HONO) Formation from the Irradiation of Aqueous Nitrate Solutions in the Presence of Marine Chromophoric Dissolved Organic Matter: Comparison to Other Organic Photosensitizers

Stephanie L. Mora Garcia, Shubhrangshu Pandit, Juan G. Navea, and Vicki H. Grassian*

Cite This: *ACS Earth Space Chem.* 2021, 5, 3056−3064

Read Online

ACCESS | Metrics & More | Article Recommendations | Supporting Information

ABSTRACT: Nitrous acid (HONO), a highly reactive trace atmospheric gas, is often underestimated in global atmospheric models due to the poor understanding of its sources and sinks, especially in the marine boundary layer (MBL). Herein, we have investigated HONO formation from the irradiation of nitrate solutions in the presence of increasingly complex photosensitizers including marine dissolved organic matter (m-DOM), which contains chromophoric organic matter, collected from a large-scale mesocosm experiment. In particular, aqueous nitrate solutions in the presence of m-DOM, humic acid (HA), and 4-benzoylbenzoic acid (4-BBA) as well as ethylene glycol (EG) were irradiated with a solar simulator. Gas-phase HONO and NO_2 produced during the irradiation of these samples were detected using incoherent broad band cavity enhanced absorption spectroscopy (IBBCEAS). The relative amounts of HONO and NO_2 formation varied for the different samples. The addition of all of these different organic containing samples (m-DOM, HA, 4-BBA, and EG) to nitrate solutions caused an enhancement in HONO formation, with m-DOM showing the greatest total amount over a 6 h time period. Mechanisms for this enhancement are discussed as well as the strong pH dependence, with the greatest amount of HONO at a low pH. Overall, HONO formation from nitrate photolysis in the presence of m-DOM provides insights into the HONO formation pathway in the MBL and ultimately contributes to improving atmospheric models.

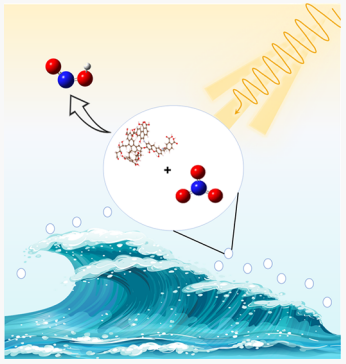

KEYWORDS: *nitrous acid (HONO), sea spray aerosol, marine dissolved organic matter (m-DOM), nitrate photochemistry, photosensitizer, marine boundary layer (MBL)*

INTRODUCTION

Trace chemical oxidizers like nitrous acid (HONO) are highly reactive and, as such, play a large role in the chemistry of the atmosphere. Reactions that lead to nitrous acid formation have been studied extensively for over the past 30 years due to the rapid photolysis of HONO into OH and NO at wavelengths between 300 and 400 nm, which falls within the solar spectrum as well as some indoor light sources, relevant to photochemistry in indoor environments.[1−6] It has been reported that, in some conditions, HONO photolysis can be the major source of OH formed outdoors.[7] Understanding sources of OH is important as it is the most significant oxidant in the atmosphere[8] and contributes to the oxidation of volatile organic carbons (VOCs) to form secondary organic aerosols.[7,9]

There are many reaction pathways that lead to the formation of HONO in the atmosphere, which can be separated into two categories: nighttime and daytime sources. Nighttime sources include direct emissions from soil bacteria, as well as reactions that occur in the absence of a light source, such as the hydrolysis of NO_2 in the presence of adsorbed water.[10,11] Daytime sources include aqueous and particulate nitrate photolysis and the photosensitized reduction of NO_2 in the presence of organic chromophores.[12−15]

In recent years, HONO has been measured in clean marine boundary layer (MBL) environments where there is no significant influence from pollution, and maximum values have been found at noon, highly suggesting that photochemical sources are of great significance.[4,16] The measurements of HONO in the MBL along with complementary modeling analysis indicated that the most likely source of HONO is due to the photosensitized reduction of NO_2 or particulate nitrate photolysis, with the latter being more common.[16−18] Furthermore, although previous models of the NO_x cycle have treated HNO_3 as a sink, recent models, including work from Ye et al., have incorporated particulate nitrate as a daytime source of HONO.[17] It is well-known that the displacement reaction of chloride in sodium chloride, a

Special Issue: Mario Molina Memorial

Received: August 17, 2021
Revised: October 9, 2021
Accepted: October 12, 2021
Published: November 2, 2021

https://doi.org/10.1021/acsearthspacechem.1c00292
ACS Earth Space Chem. 2021, 5, 3056−3064

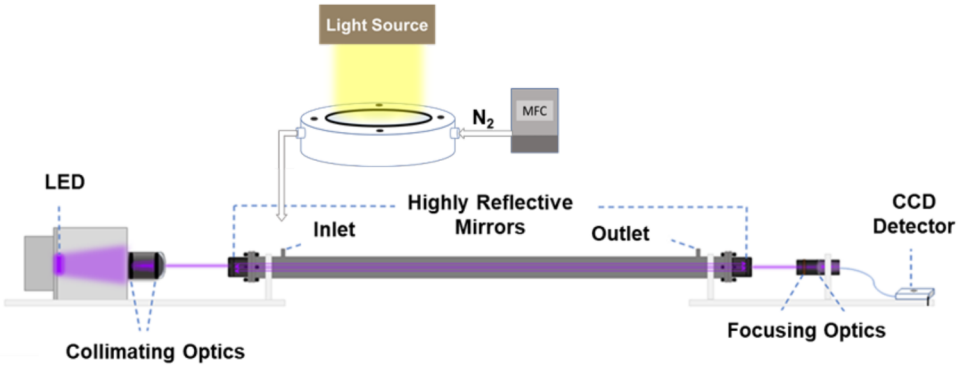

Figure 1. Schematic of the IBBCEAS used for NO_2 and HONO detection. The aqueous sample cell is irradiated with a solar simulator. A continuous flow of nitrogen guiding the gases produced from the irradiation of the nitrate containing solutions above the sample is sent into the cavity. LED = light emitting diode, MFC = mass flow controller, CCD = charged coupled device.

component of sea spray aerosol (SSA), with nitrate, from nitric acid and other nitrogen oxides, in polluted atmospheres leads to sodium nitrate.[19,20] Furthermore, SSA have also been shown to contain organics compounds including aliphatic molecules such as fatty acids and amino acids and condensed aromatics that can act as photosensitizers,[21,22] and as noted above, the presence of these can enhance HONO formation. All of this suggests that aged SSA in the MBL could be a source of HONO.

Laboratory studies can provide insights into the mechanisms and kinetics of HONO formation; therefore, we have investigated the photochemistry of nitrate solutions to represent aged sea spray aerosols, in the presence of different photosensitizers and organic compounds to elucidate information into the relevant environmental conditions leading to HONO formation. Specifically, we have focused on measurements of gas-phase NO_2 and HONO produced from the simulated solar irradiation of nitrate in the presence of marine dissolved organic matter (m-DOM) collected from a large-scale mesocosm campaign, SeaSCAPE.[23] We compared these results to nitrate solutions in the presence and absence of humic acid (HA), 4-benzoylbenzoic acid (4-BBA), and ethylene glycol (EG). HA has been used as a terrestrial proxy for m-DOM in many heterogeneous and photochemical studies, though recently it was deemed as not a good proxy in a comparison study.[22] 4-BBA has also been used as a much simpler chemical proxy when studying photochemical sources of HONO and is a derivative of benzophenone, a commonly used photosensitizer, and also a proxy for light absorbing components within m-DOM.[7,22] EG has been used in studies as a hydroxyl radical scavenger and found to also lead to an enhancement of HONO formation in the nitrate photolysis pathway.[12] These complementary measurements were used to help elucidate the enhancement mechanisms of HONO when m-DOM is present.

Additionally, the impact of pH was explored on the relative yields of NO_2 and HONO. Previously, Scharko et al. found that aqueous nitrate photolysis is a viable source of gaseous HONO and NO_2 at pH values lower than 3.2, the pK_a value for HONO.[12] Relevant to this current study is the measurements of Angle et al. that showed that SSA produced from ocean waters can easily become acidified to values between pH 2 and 4 depending on size.[24] Therefore, experiments conducted in this work on the irradiation of nitrate solutions at a low pH give insights into HONO and NO_2 formation in aqueous SSA aerosols due to nitrate photolysis and the effects of organics when present.

EXPERIMENTAL SECTION

Incoherent Broadband Cavity Enhanced Absorption Spectroscopy (IBBCEAS). The simultaneous and quantitative measurements of gaseous HONO and NO_2 that formed in these studies were accomplished using an in-house designed and constructed incoherent broadband cavity enhanced absorption spectrometer (IBBCEAS).[5,25] A simple schematic of the instrument is shown in Figure 1. The spectrometer consists of a 75 cm long cavity made of polytetrafluoroethylene (PTFE) with an inner diameter of 2.5 cm. High reflectivity mirrors are mounted on optics holders both from CRD optics with micrometer adjustments (mirrors, 99.99% reflectivity at 370 nm, ROC = 1 m, diameter = 2.54 cm; holders, model number 902-8010). Closing caps attached to each of the mounts have inlet tubes to introduce N_2 as a purge gas to keep the mirrors clean. There are inlet and outlet ports at both ends of the cavity. The nitrogen flow containing the trace gases flows through these ports and is set using mass flow controllers. Atmospheric pressures are maintained inside the cavity.

The IBBCEAS light source used is a Nichia Laboratories UV LED (NVSU333A, 3.640 W) that emits from 360 to 390 nm with a peak at 365 nm. It is mounted on a copper printed circuit board (Cree XHP-70 MCPB), which is attached to a copper plate to dissipate heat. This copper plate is further cooled by a Peltier cooler attached to an Arctic Alpine 11 plus CPU fan. To further decrease thermal heating, the copper plate is placed inside a custom aluminum housing that allows for movement in the xy and yz planes. The power output for the LED and Peltier cooler are controlled using a custom Labview program and custom circuit board interfaced with a National Instruments MyRIO device.

To align and collimate the light from the LED, the housing also contains an optics holder where two aspheric condenser lenses (Thorlabs, ACL25416U-A, diameter = 1 in., NA = 0.79) are placed to direct the collimated light into the first mirror and then the cavity. On the other end of the cavity, a bandpass filter (Semrock, FF01-370/36-25, 25 mm) is first used to eliminate light outside the range 300−400 nm. This filtered light is directed onto a focusing lens (Thorlabs, LA4380-UV, diameter = 1 in., AR coated 245−400 nm, f/3.93, focal length = 100 mm) with a focal point of 10 cm onto a fiber optic (Ocean optics, PL100-2-UV−vis, diameter

https://doi.org/10.1021/acsearthspacechem.1c00292
ACS Earth Space Chem. 2021, 5, 3056−3064

= 1 mm, NA = 0.22) leading to a CCD detector (Ocean Optics QEPro) with a 25 nm entrance slit. The resolution of the spectrometer was determined to be 0.9 nm. Spectra are taken using the accompanying software to the OceanOptics detector.

The experimental setup gives an average effective path length in the cavity of 1.05 km across the spectral region from 360 to 390 nm with a maximum of 1.57 km at the higher wavelength region. The reflectivity and effective path length are determined by comparing the loss of light due to Rayleigh scattering by He and N_2; this calculation can be found in the Supporting Information. To validate the instrument, the r^2 value of the actual NO_2 concentration versus instrument derived NO_2 concentration in the range from 50 to 125 ppb was determined to be 0.96.[5]

Reaction Cell, Solar Irradiation Experimental Setup, and Solution Preparation. A reaction cell was custom-made of PTFE to minimize a wall loss of HONO; a schematic of the experimental setup is shown in Figure 1. The reaction cell is custom-built, can hold 7 mL of liquid solution, and has a headspace volume of 40 mL. The inlet and outlet fittings are in line with each other so as to ensure there is no unnecessary increase of residence time of the gaseous products in the cell. The top of the sample holder is fit with a 17.35 cm^2 quartz window. The mount is kept in place through a set of screws holding the top and bottom parts of the reaction cell together. The carrier gas, Praxair UHP nitrogen, is guided into the cell at 100 sccm with PTFE 1/4" tubing and is directed into the inlet of the cavity. After the reaction cell, all tubing is wrapped with black electrical tape to avoid light exposure. Directly after the reaction cell is a PTFE Pellparts (PN 4251) aerosol filter to avoid water droplets in the lines and in the cavity. The reaction cell rests on top of aluminum blocks, which are in direct contact with the metal laser table to dissipate any heat from the solar simulator.

A Newport (67005) solar simulator with a Xenon Arc lamp with the spectral output shown in Figure S2 was used to irradiate the samples. The reaction cell is placed 5 cm from the output to reach an irradiation intensity of 1 sun (1000 Wm^{2-}). A water filter is placed in between the reaction cell and the solar simulator and cooled with a flowing water cooler to filter out IR radiation.

All experiments were carried out in aqueous solutions of sodium nitrate with added organics and acidified to the desired pH as described in more detail below. The m-DOM used was collected from the NSF-SeaSCAPE 2019 campaign.[23] The desired concentration of m-DOM was created by weighing the dried sample and then placing in Milli-Q water and dissolving the mixture by sonication for 3 h. Humic acid used was Suwannee River humic acid from the International Humic Substance Society, 4-BBA was from Sigma-Aldrich, and the ethylene glycol used was from Fisher Chemicals. Both m-DOM and HA were used at a concentration of 0.1 mg/mL. The concentration used for 4-BBA and ethylene glycol was 0.44 mM, which is equivalent to 0.1 mg/mL 4-BBA. After dissolving the m-DOM in MQ water, the desired amount of Sigma-Aldrich $NaNO_3$ was added and sonicated for an additional 5 min. Once this was completed, the pH was adjusted to the desired pH with dilute HCl. The pH for the comparison studies of the effects of the organics was adjusted to 2.0, to stay below the pK_a of HONO. For the pH studies with m-DOM present, the pH was adjusted to 2.0, 3.0, 3.5, 4.0, and 7.0.

Determination of Gas-Phase HONO and NO_2 Concentrations. Prior to the beginning of the experiments, the cavity, reaction cell, and all lines were evacuated of any HONO or NO_2 by flowing N_2 for at least an hour. Following this, an off period prior to irradiation was acquired for an hour followed by the acquisition of spectra for 5 h of irradiation and 5 h after irradiation. The spectra were averaged 10 times and were integrated for 20 s, giving information every 200 s. The data were deconvoluted and analyzed using the Differential Optical Absorption Spectroscopy Intelligent System (DOASIS) software.[26] The software fits the experimental data and separates the contribution from different components of the gas mixtures from the transmittance into the absorption due to HONO and NO_2 by comparing them to their respective cross section reference spectra, and the rest is fit to a polynomial.[27,28] More information on this can be found in a previously published paper.[5]

RESULTS AND DISCUSSION

Gas-Phase HONO and NO_2 from Irradiated Nitrate Solutions. To get a baseline concentration of HONO formation from nitrate photolysis without the organic compounds present, an acidic aqueous nitrate solution at pH 2 was irradiated and the gaseous HONO and NO_2 was measured. Figure 2A shows the formation of HONO while the solutions were irradiated. After 2 h, the HONO formation plateaued around 80 ppb. Figure 2B shows the immediate formation of NO_2, which occurs within the first 200 s following irradiation by the solar simulator. In contrast to the HONO time course measurements, NO_2 concentrations increase sharply upon the irradiation with the solar simulator and decrease sharply when irradiation ceases. This behavior for NO_2 formation is also seen when organics are present in the solutions.

The presence of organic compounds significantly enhances HONO concentrations by a factor of 2−5. In contrast, NO_2 concentrations decrease in the presence of organic compounds by 0.6−0.9 times that of the pure nitrate solution. In the presence of m-DOM, HONO formed up to an average 425 ppb once it reached a steady state, which occurs 2 h after the start of irradiation. Figure 3 shows that, at the period in which the maximum amount of HONO was formed, NO_2 was detected at about 100 ppb. When comparing the values of HONO and NO_2 with and without m-DOM present, m-DOM enhances HONO by a factor of ca. 5 and the amount of NO_2 decreased by 10%. Figure 3 shows that 4-BBA had a HONO enhancement factor of ca. 3. In comparison to the different compounds added to the nitrate solutions, 4-BBA had lowest enhancement, but it is still significantly more HONO than that measured from pure sodium nitrate solutions without the presence of organic compounds. Additionally, Figure 2B shows that 4-BBA had the lowest amount of NO_2, with the concentration being 0.6 times the amount measured in the nitrate solution alone. Interestingly for EG containing solutions, the time profile for the HONO during irradiation differed in shape compared to those of other solutions (Figure 2A). EG also showed an enhancement factor of 3.6 at 2 h of irradiation (Figure 3). The solutions with EG were the only ones that did not reach a steady state emission of HONO at 2 h of irradiation; instead,

https://doi.org/10.1021/acsearthspacechem.1c00292
ACS Earth Space Chem. 2021, 5, 3056−3064

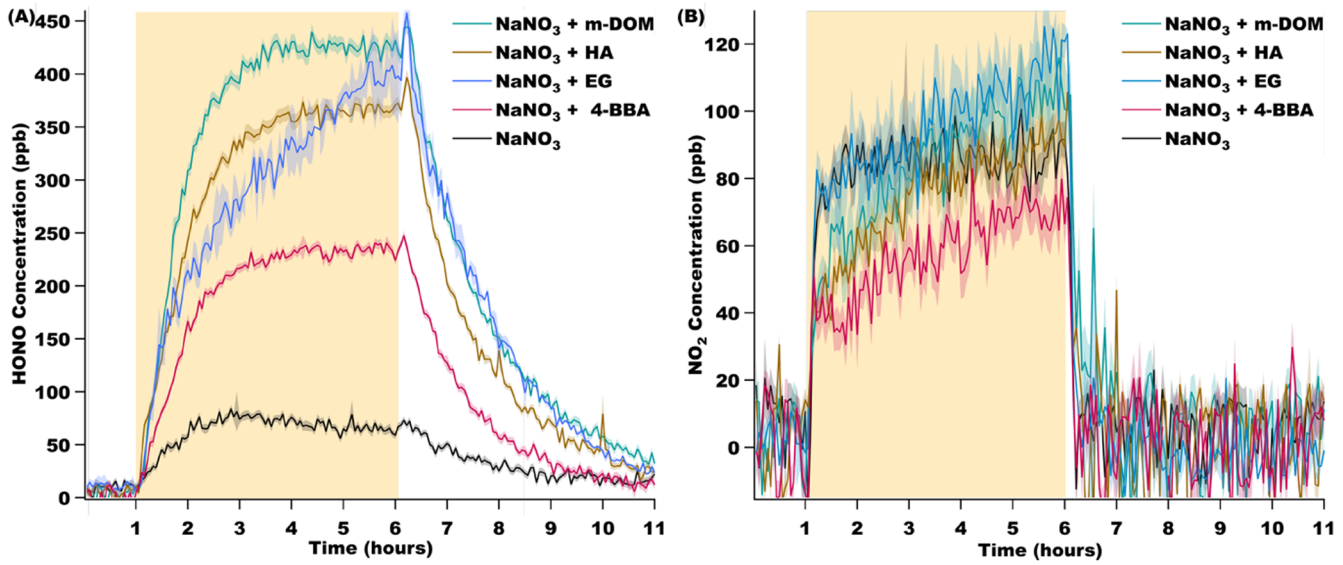

Figure 2. Time course profiles of (A) HONO and (B) NO_2 concentrations (in ppb) detected for solutions with 100 mM $NaNO_3$ in the presence of different organic compounds. The yellow box indicates when solutions were irradiated with the solar simulator. The error displayed on the figure as shading is one standard deviation calculated from triplicate experiments. For HONO values above the limit of detection, the error is an average of 4% of the HONO values for each point, and for NO_2, it is an average of 10% (note: m-DOM = marine dissolved organic matter, teal; HA = humic acid, brown; EG = ethylene glycol, blue; and 4-BBA = 4-benzoylbenzoic acid, pink).

HONO concentrations increased steadily for the entire time the sample was irradiated with the solar simulator. Lastly, humic acid had a similar HONO formation profile to m-DOM and 4-BBA and had an enhancement factor of ca. 4, whereas the amount of NO_2 measured at the 2 h irradiation point decreased and was 0.8 times that of the pure sodium nitrate solution.

Surface Tension Measurements. To better understand the surface activity of these various organic compounds, the surface tensions were measured. Table 1 displays the surface tension measurements of the organic solutions at 1 mg/mL without nitrate present. Samples containing EG, HA, and 4-BBA show very similar surface tensions as Milli-Q water; however, samples containing m-DOM showed a marked decrease in the surface tension with a value of 65.9 ± 0.5 mN/m. Thus, components within m-DOM are highly surface active. HA has been found to lower the surface tension of aqueous solutions due to the amphiphilic functional groups.[29] Compared to HA, the m-DOM solution has a lower surface tension, suggesting that m-DOM is composed of more surface-active molecules than HA. This surface activity can impact the degassing of HONO and NO_2. Table 1 and Figure 3 show that solutions containing m-DOM, the organic photosensitizer with the highest surface activity, yields the largest amount of HONO. Ongoing studies are investigating the concentration dependence of HONO formation with m-DOM to determine the impact on the rate and yield of HONO with decreasing surface tension.

Interestingly, solutions with EG were the only ones that slightly increased in surface tension compared to pure water. In general, there is no effect in the degassing of products as there is no microlayer of organics at the surface of the solutions containing EG. This suggests that the slow decrease of HONO concentration after the irradiation period (Figure 2A) is mostly due to a slower HONO formation rather than a slow degassing of products. The higher surface activity that m-DOM and HA introduce affects the rate of degassing for

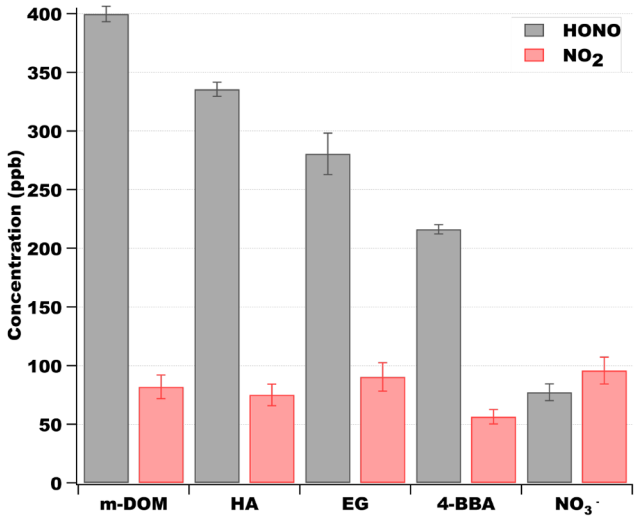

Figure 3. HONO (gray bars) and NO_2 (red bars) concentrations (in ppb) at 2 h of irradiation for the different nitrate solutions. The bin labeled NO_3^- is just the sodium nitrate solution without any organic compounds added to the solution and the other bins labeled for organics present with nitrate (m-DOM = marine-dissolved organic matter; HA = Suwannee River humic acid; EG = ethylene glycol; 4-BBA = 4-benzoylbenzoic acid). The error bars represent the experimental error, which was found to be the largest source of error. For HONO in this region, the error was about 4% of total HONO values and 10% for NO_2 (see the Supporting Informatio (SI) for more information).

HONO and NO_2 differently. HONO slowly increases and decreases for all the solutions, including the ones without the presence of an organic, whereas NO_2 promptly, within seconds, responds to irradiation. In a previous study, Reeser et al. reported seeing a significant change in both the degassing profiles and steady state concentrations of NO_2 detected after the irradiation of aqueous nitrate solutions in

https://doi.org/10.1021/acsearthspacechem.1c00292
ACS Earth Space Chem. 2021, 5, 3056−3064

Table 1. Surface Tension Values of the Solutions Used in the Experiments[a]

organic present	surface tension without the presence of $NaNO_3$ (mN/m)
none/Milli-Q water	72.8 ± 0.1
EG	73.1 ± 0.1
4-BBA	72.3 ± 0.2
HA	72.3 ± 0.1
m-DOM	65.9 ± 0.5

[a]m-DOM = marine-dissolved organic matter; HA = Suwannee River humic acid; EG = ethylene glycol; 4-BBA = 4-benzoylbenzoic acid

the presence of organic monolayers on the surface of the solutions, and it was concluded that the difference was likely due the orientation of molecules at the interface, inhibiting surface adsorption and/or degassing of NO_2.[30] In the current study, there was no detectable change in the degassing of NO_2 with regards to the different organics present but there was for HONO, specifically the different profiles of HONO evolution. Additionally, the different kinetic profiles found for the different organics present signify that interactions with the walls of the experimental setup are not the main contributing factor for slow HONO kinetics.

Mechanisms for HONO Enhancement in the Presence of Organic Compounds and Complex Organic Samples (m-DOM, HA, 4-BBA, and EG). Without the presence of organics, the irradiation of the acidified aqueous nitrate solutions leads to the formation of HONO and NO_2. Interestingly, NO_2 was not measured at an order of magnitude higher than that of HONO, in contrast to what the nitrate photolysis mechanism shown in Scheme 1A Reactions 1 and 2 suggests due to the associated quantum yields.[31] Scharko et al. similarly reported a HONO/NO_2 ratio of about 1:1 for acidic sodium nitrate solutions as seen in Figure 3.[12] Likely, as nitrite is turned into HONO after protonation in the acidic solutions, it drives the nitrite forming reaction forward (Reaction 2) leading to more HONO formation. As noted previously, HONO increases and decreases slowly after irradiation stops. This is presumably due to the additional protonation step of NO_2^- to form HONO.

Introducing organics increased the measured amount of HONO, with m-DOM being the most efficient. m-DOM, a complex mixture of condensed aromatics (and or other light absorbing components) and aliphatic components, has the ability to enhance HONO formation via different pathways, including photosensitized reactions and another via other secondary reactions.[22,32−34] Measuring HONO formation of irradiated sodium nitrate samples with m-DOM gives information on the significance of m-DOM for enhancing yields of HONO as it pertains to the MBL, but it gives little information regarding the potential enhancement mechanisms.

Marine dissolved organic matter contains a significant amount of aliphatic compounds that have been proposed to enhance HONO formation in a nonphotochemical pathway.[22,32] Aliphatic compounds will form superoxide radicals by reacting with OH in solution, a reaction that depends on the presence of dissolved oxygen.[35−37] These radicals then have secondary reactions with any NO_2 or NO solvated in the solutions that lead to an enhanced amount of HONO.[38−40] Ethylene glycol was chosen to probe this

Scheme 1. Mechanisms for HONO Production[a]

A. Nitrate photolysis

1) $NO_3^-{}_{(aq)} \xrightarrow{h\nu} NO_2^-{}_{(aq)} + O(^3P)\ \Phi=0.001$

2) $NO_3^-{}_{(aq)} \xrightarrow{h\nu\ H^+} NO_2 + OH\ \Phi=0.01$

3) $NO_2^-{}_{(aq)} + H^+ \rightarrow HONO_{(g)}$

B. Secondary reactions with superoxide radical

4) 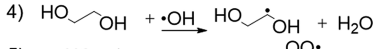

5) 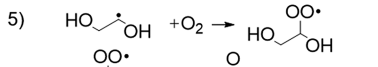

6) 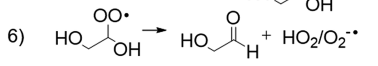

7) $O_2^{-\bullet} \xrightarrow{NO_2} OONO_2^- \rightarrow O_2 + NO_2^-$

8) $O_2^{-\bullet} \xrightarrow{NO} OONO^- \underset{}{\overset{pKa\ 6.5}{\rightleftharpoons}} OONOH$

9) $OONO^- + OONOH \rightarrow O_2 + 2NO_2^- + H^+$

C. Aqueous electron reduction

10) $^1m\text{-}CDOM \xrightarrow{h\nu} {}^1m\text{-}CDOM^{+/-\bullet}$

11) $^1m\text{-}CDOM^{+/-\bullet} \rightarrow {}^1m\text{-}CDOM^{+\bullet} + e^-_{(aq)}$

12) $e^-_{(aq)} + NO_3^-{}_{(aq)} \rightarrow NO_2^-{}_{(aq)} + O^-$

13) $e^-_{(aq)} + O_{2(aq)} \rightarrow O_2^{-\bullet}$

D. Release of hydroxyl radical from irradiated m-CDOM

14) $^1m\text{-}CDOM \xrightarrow{h\nu} {}^3m\text{-}CDOM^*$

15) $^3m\text{-}CDOM^* + H_2O \rightarrow m\text{-}CDOM\text{-}H + {}^\cdot OH$

[a](A) Nitrate photolysis in acidic aqueous solutions. (B) Secondary reactions involving the superoxide radical. (C) Aqueous electron reduction. (D) Formation of ROS (hydroxyl radicals) from the irradiation of m-CDOM.

mechanism; any enhancement that is observed is assumed to be from secondary reactions with superoxide. In Scheme 1B, proposed mechanisms from Wang et al. were adapted to incorporate ethylene glycol as the molecule that leads to the superoxide radical (Scheme 1C Reactions 4−6).[38] Reactions 7−9 in Scheme 1B show that NO_2 and NO present in the solution react with the superoxide radical to form more nitrite. This leads to an increase in nitrite in the solution, which leads to more HONO (Scheme 1A Reaction 3). Interestingly, Figure 2B shows more NO_2 detected in this solution compared to that with just sodium nitrate present for irradiation times over two hours. It is possible that the secondary reactions consuming the NO_2 and NO drive Reaction 2 forward. In turn, this may be what causes the different profiles for HONO and NO_2 as well as the highest NO_2 concentrations measured after 2 h of light exposure. Additionally, the slower formation of HONO may be attributed to the requirement of more reaction steps to occur to lead to the enhancement or the effect of the surface interactions leading to a slower degassing.

To probe the contribution due to the light absorbing, or chromophoric, components of m-DOM (m-CDOM), the enhancement due to 4-BBA, a highly conjugated molecule, was also investigated. The literature has proposed that the highly conjugated m-DOM systems can absorb light and undergo a radical charge separation, leading to an aqueous electron (Scheme 1C Reactions 10 and 11).[34] With nitrate present in the solution, we are proposing that the aqueous electron reduces nitrate into nitrite, as shown in Scheme 1C

https://doi.org/10.1021/acsearthspacechem.1c00292
ACS Earth Space Chem. 2021, 5, 3056−3064

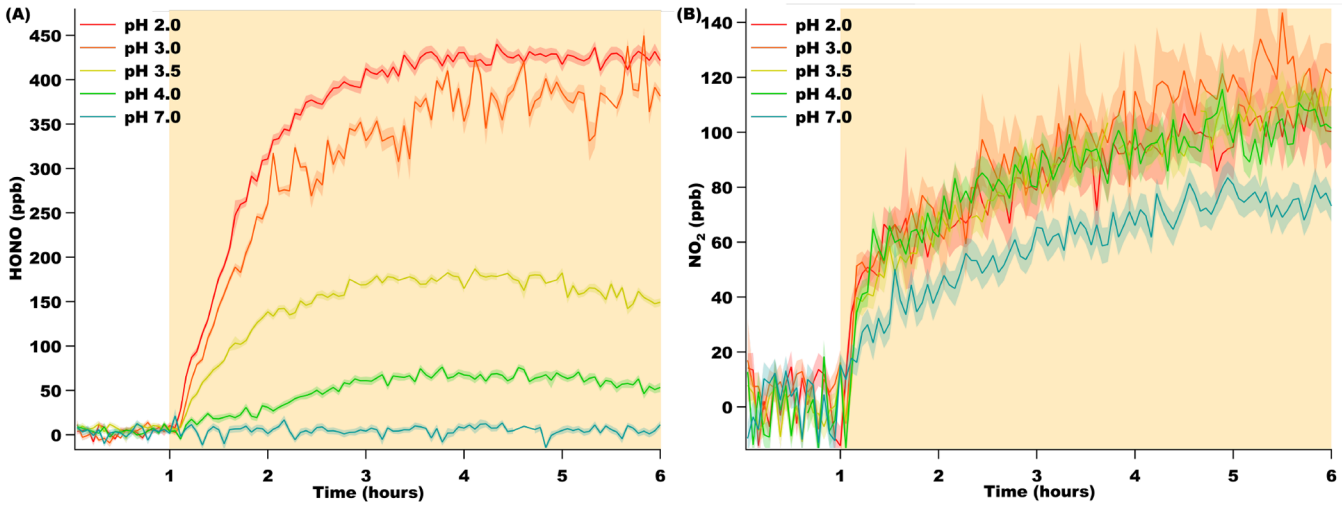

Figure 4. (A) HONO and (B) NO_2 values for 100 mM $NaNO_3$ + 0.1 mg/mL m-DOM solutions at varied pH values. The concentrations of HONO and NO_2 are on the *y*-axis in parts per billion, and the time in hours is on the *x*-axis. The irradiation period is denoted by the highlighted yellow region.

Reaction 12. An enhanced amount of nitrite in an acidic solution would protonate and lead to more gaseous HONO, as shown in Reaction 3. The molecular compound 4-BBA was chosen as a proxy that would undergo a similar mechanism; a molecule specific mechanism can be found in Scheme S1. It is highly conjugated and has the carbonyl group that can charge separately after being in the triplet state, like that shown for m-CDOM in Scheme 1C.[22,41] The solutions with 4-BBA present were the only ones that showed a significant difference in the amount of NO_2 measured and that can be understood by Scheme 1C. As nitrate is decreased in the solution, less would be available to form NO_2 via the nitrate photolysis reaction in Scheme 1A Reaction 2. However, when solvated electrons are in an aqueous solution, the more likely reaction to occur is Reaction 13 where the electron will form the superoxide radical when it reacts with dissolved oxygen.[37] In this scenario, the photochemical formation of the solvated electron further enhances HONO formation by feeding into reaction Scheme 1B Reactions 7−9 due to the increase in superoxide radical.

Humic acid thin films have been studied as a possible source of HONO via the photosensitized reduction of NO_2. Though it has been shown that HA is not an appropriate chemical proxy for m-DOM, mainly due the compositional differences, it was also used in this study as it is a complex system that has both chromophores and other components that are not light absorbing.[22] Previous studies of HONO formation from HA have flowed NO_2 over thin films of HA.[7,13,42,43] In the presented study, this mechanism is less likely because HA is not present in a thin film, and as seen in Figure 2A,B, there is an increase of HONO detected but no corresponding decrease NO_2 detected. If HONO was being formed via this pathway, a decrease of NO_2 would also be observed. Furthermore, given that the amount of nitrate in solution is much greater, the nitrate photochemistry pathway (Scheme 1A) would be more favorable. HA has been found to have high amounts of ketone, carboxylic, aromatic, and aliphatic functional groups like m-DOM.[44] However, a comparative study of HA and m-DOM found that there are compositional differences.[22] HA has a lower nitrogen content, but was found to have more aromatic, condensed aromatic, and aliphatic function groups. Additionally, HA displayed a lower photosensitization efficiency compared to m-DOM. A lower photosensitization efficiency may mean there is a lower triplet state efficiency. Future studies are designed to probe these mechanisms in greater detail.

Marine dissolved organic matter and humic acid are complex organic systems that contain many compounds including aliphatic compounds and light absorbing, chromophoric compounds, so it is likely the enhancement of HONO that is measured is due to multiple enhancement pathways. In addition to an increase of superoxide radicals, it has been shown that the irradiation of m-DOM and isolates like humic acid will form hydroxyl radicals via different reaction pathways.[34] Scheme 1D shows the proposed pathway of the H abstraction of water by triplet state m-DOM (^{3}m-DOM*) following excitation to the singlet state (^{1}m-DOM*) and subsequent intersystem crossing (Reactions 14 and 15).[45] Other photochemical mechanisms of hydroxyl radical formation include the photolysis of hydrogen peroxide, which has also been measured in irradiated m-DOM samples,[46,47] low energy hydroxylation, and photo-Fenton reactions, all of which are discussed in detail by McKay and Rosario-Ortiz.[45] The enhancement in hydroxyl radicals with aliphatics present in m-DOM would further enhance Scheme 1B starting at Reaction 4. The OH secondary mechanism (Scheme 1B) and the photochemical production sources of $O_2^{\bullet -}$ and •OH (Scheme 1C,D), which feed into Scheme 1B, are all significant pathways for the enhancement of HONO when m-DOM and HA are present in aqueous nitrate solutions. A comparison of HONO formation with EG and 4-BBA present suggests that nonphotochemical superoxide formation might be greater than the photochemical formation of superoxide and hydroxyl radicals. However, it is important to note that EG and 4-BBA may not be the most efficient molecular models to show the enhancements of each enhancement mechanism. Nevertheless, seeing that m-DOM has a larger enhancement of HONO formation is important and suggests that marine organic compounds play an important role in HONO formation in the MBL.

https://doi.org/10.1021/acsearthspacechem.1c00292
ACS Earth Space Chem. 2021, 5, 3056−3064

HONO Formation Probed as a Function of pH. In addition to organic content of SSA, the pH of the aerosol is another factor that must be considered with regards to how it affects the HONO formation efficiency from nitrate photolysis due to the need of excess protons to protonate the nitrite ion in solution into gaseous HONO. The role of pH was previously studied for aqueous nitrate solutions by Scharko et al.[12] In the current study, the dependence of pH on HONO and NO_2 formation was also investigated in the presence of m-DOM. Figure 4 shows that, at pH 2 and 3, a high amount of HONO is detected but at pH 3.5 it begins to decrease significantly. Even less is detected at pH 4 and at pH 7. This is due to the pH being above the pK_a of HONO, causing nitrite to remain deprotonated and remaining in the solution. Interestingly, at pH 7, NO_2 decreases, which was not the case for any of the other pH ranges. Reaction 2 of Scheme 1A shows that free protons are required for the reaction that forms NO_2 to progress because it is needed to form the secondary product, OH. This suggests that pH is more important for HONO formation than it is for NO_2, but most importantly, it informs that the HONO/NO_2 ratio can change as a function of pH. Recent measurements by Angle et al. have shown that SSA is quite acidic upon formation. Total suspended aerosol pH measurements, which is a measure of the mostly supermicron sized particle, found a pH of 4, whereas for submicron SSA, a value of 2 was measured.[24] These measurements of HONO and NO_2 as a function of SSA pH show that, in the conditions chosen for this study, HONO formation is favorable over NO_2.

CONCLUSION AND ATMOSPHERIC IMPLICATIONS

The main goal of this study was to gain insight into the sources of HONO in the marine boundary layer during the day. The findings suggest that aged sea spray aerosols that contain nitrate and m-DOM are likely a significant contributor to the elevated amounts of measured HONO in the MBL during the daytime. m-DOM from the NSF-SeaSCAPE 2019 mesocosm campaign was found to enhance HONO formation the most compared to commonly used model systems humic acid and 4-benzoylbenzoic acid as well as the nonchromophoric ethylene glycol. It is proposed that m-DOM enhances HONO formation via one pathway, which is the secondary reaction of the superoxide radical with NO_2 and NO. This pathway can be enhanced photochemically by the formation of superoxide radicals when solvated electrons are formed by the charge splitting of excited m-DOM and are in the presence of water and by the formation of hydroxyl radicals from the irradiation of m-DOM. These enhancement pathways lead to higher levels of nitrite in the solution, leading to elevated HONO formation.

These results support observations of HONO in the MBL where HONO concentrations are seen to display a diurnal cycle with a peak at noon. Nitrate photochemistry within SSA has been proposed to be the source, and this current study gives insight into how marine organics present within SSA can enhance HONO formation from nitrate photolysis. This is the first study to use a complex m-DOM sample and compare it to commonly used model systems as well as other complex samples such as HA. Furthermore, this study aids in the overall picture of HONO production in the atmosphere. These findings can inform atmospheric chemistry models to better understand and predict HONO formation in the MBL.

ASSOCIATED CONTENT

Supporting Information

The Supporting Information is available free of charge at https://pubs.acs.org/doi/10.1021/acsearthspacechem.1c00292.

Discussions of incoherent broadband cavity enhanced absorption spectroscopy, solar simulator output used for broadband irradiation, radical charge separation in 4-BBA, largest source of error in the IBBCEAS data, and verification that HONO and NO_2 formation is due to nitrate photolysis, figures of wavelength dependent reflectivity, calculated effective pathlength, overlap in the solar simulator photon flux and absorption spectrum, concentration of HONO, and HONO and NO_2 concentrations, and scheme of reaction pathway (PDF).

AUTHOR INFORMATION

Corresponding Author

Vicki H. Grassian − *Department of Chemistry and Biochemistry, University of California San Diego, La Jolla, California 92037, United States;* orcid.org/0000-0001-5052-0045; Email: vhgrassian@ucsd.edu

Authors

Stephanie L. Mora Garcia − *Department of Chemistry and Biochemistry, University of California San Diego, La Jolla, California 92037, United States;* orcid.org/0000-0001-5832-9085

Shubhrangshu Pandit − *Department of Chemistry and Biochemistry, University of California San Diego, La Jolla, California 92037, United States;* orcid.org/0000-0002-2744-9006

Juan G. Navea − *Department of Chemistry, Skidmore College, Saratoga Springs, New York 12866, United States;* orcid.org/0000-0002-7723-6033

Complete contact information is available at: https://pubs.acs.org/10.1021/acsearthspacechem.1c00292

Notes

The authors declare no competing financial interest.

Data Availability. Data for this study can be accessed in the Center for Aerosol Impacts on Chemistry of the Environment (CAICE) University of California San Diego Library Digital Collections (https://doi.org/10.6075/J0CC10V7).

ACKNOWLEDGMENTS

This work was supported by the National Science Foundation through the NSF Center for Aerosol Impacts on the Chemistry of the Environment, a Center for Chemical Innovation (CHE-1801971). The authors would like to thank Michael R. Alves for leading the effort in the large-scale collection of m-DOM from the NSF-SeaSCAPE campaign as well as his contributions to the project in the form of discussions. The authors would also like to thank Dr. Michael N. Sullivan, Dr. Kristin Wall, and Dr. Jonathan Trueblood for their guidance in early stages of the development of the instrument and experimental protocols. Finally, thanks to Prof. Mark Young and Heather Ricker for helpful discussions.

REFERENCES

(1) Alicke, B.; Geyer, A.; Hofzumahaus, A.; Holland, F.; Konrad, S.; Pätz, H. W.; Schäfer, J.; Stutz, J.; Volz-Thomas, A.; Platt, U. OH Formation by HONO Photolysis during the BERLIOZ Experiment. *J. Geophys. Res.* **2003**, *108* (4), 3−1.

(2) Ramazan, K. A.; Syomin, D.; Finlayson-Pitts, B. J. The Photochemical Production of HONO during the Heterogeneous Hydrolysis of NO_2. *Phys. Chem. Chem. Phys.* **2004**, *6*, 3836−3843.

(3) Kleffmann, J. Daytime Sources of Nitrous Acid (HONO) in the Atmospheric Boundary Layer. *ChemPhysChem* **2007**, *8* (8), 1137−1144.

(4) Ye, C.; Zhou, X.; Pu, D.; Stutz, J.; Festa, J.; Spolaor, M.; Tsai, C.; Cantrell, C.; Mauldin, R. L.; Campos, T.; et al. Rapid Cycling of Reactive Nitrogen in the Marine Boundary Layer. *Nature* **2016**, *532* (7600), 489−491.

(5) Pandit, S.; Mora Garcia, S. L.; Grassian, V. H. HONO Production from Gypsum Surfaces Following Exposure to NO_2 and HNO_3: Roles of Relative Humidity and Light Source. *Environ. Sci. Technol.* **2021**, *55* (14), 9761−9772.

(6) Perner, D.; Platt, U. Detection of Nitrous Acid in the Atmosphere by Differential Optical Absorption. *Geophys. Res. Lett.* **1979**, *6* (12), 917−920.

(7) Han, C.; Yang, W.; Wu, Q.; Yang, H.; Xue, X. Heterogeneous Photochemical Conversion of NO_2 to HONO on the Humic Acid Surface under Simulated Sunlight. *Environ. Sci. Technol.* **2016**, *50* (10), 5017−5023.

(8) Stutz, J.; Alicke, B.; Neftel, A. Nitrous Acid Formation in the Urban Atmosphere: Gradient Measurements of NO_2 and HONO over Grass in Milan, Italy. *J. Geophys. Res.* **2002**, *107* (22), LOP 5-1.

(9) Hofzumahaus, A.; Rohrer, F.; Lu, K.; Bohn, B.; Brauers, T.; Chang, C.; Fuchs, H.; Holland, F.; Kita, K.; Kondo, Y.; et al. Amplified Trace Gas Remocal in the Troposphere. *Science* **2009**, *324*, 1702−1705.

(10) Oswald, R.; Behrendt, T.; Ermel, M.; Wu, D.; Su, H.; Cheng, Y.; Breuninger, C.; Moravek, A.; Mougin, E.; Delon, C.; et al. HONO Emissions from Soil Bacteria as a Major Source of Atmospheric Reactive Nitrogen. *Science* **2013**, *341* (6151), 1233−1235.

(11) Finlayson-Pitts, B. J.; Wingen, L. M.; Sumner, A. L.; Syomin, D.; Ramazan, K. A. The Heterogeneous Hydrolysis of NO_2 in Laboratory Systems and in Outdoor and Indoor Atmospheres: An Integrated Mechanism. *Phys. Chem. Chem. Phys.* **2003**, *5* (2), 223−242.

(12) Scharko, N. K.; Berke, A. E.; Raff, J. D. Release of Nitrous Acid and Nitrogen Dioxide from Nitrate Photolysis in Acidic Aqueous Solutions. *Environ. Sci. Technol.* **2014**, *48* (20), 11991−12001.

(13) Stemmler, K.; Ammann, M.; Donders, C.; Kleffmann, J.; George, C. Photosensitized Reduction of Nitrogen Dioxide on Humic Acid as a Source of Nitrous Acid. *Nature* **2006**, *440* (7081), 195−198.

(14) Han, C.; Yang, W.; Yang, H.; Xue, X. Enhanced Photochemical Conversion of NO_2 to HONO on Humic Acids in the Presence of Benzophenone. *Environ. Pollut.* **2017**, *231* (2), 979−986.

(15) Yang, W.; Han, C.; Yang, H.; Xue, X. Significant HONO Formation by the Photolysis of Nitrates in the Presence of Humic Acids. *Environ. Pollut.* **2018**, *243*, 679−686.

(16) Reed, C.; Evans, M. J.; Crilley, L. R.; Bloss, W. J.; Sherwen, T.; Read, K. A.; Lee, J. D.; Carpenter, L. J. Evidence for Renoxification in the Tropical Marine Boundary Layer. *Atmos. Chem. Phys.* **2017**, *17* (6), 4081−4092.

(17) Ye, C.; Zhou, X.; Pu, D.; Stutz, J.; Festa, J.; Spolaor, M.; Tsai, C.; Cantrell, C.; Mauldin Iii, R. L.; Campos, T.; et al. Rapid Cycling of Reactive Nitrogen in the Marine Boundary Layer. *Nature* **2016**, *532*, 489−491.

(18) Wen, L.; Chen, T.; Zheng, P.; Wu, L.; Wang, X.; Mellouki, A.; Xue, L.; Wang, W. Nitrous Acid in Marine Boundary Layer over Eastern Bohai Sea, China: Characteristics, Sources, and Implications. *Sci. Total Environ.* **2019**, *670*, 282−291.

(19) Ault, A. P.; Guasco, T. L.; Ryder, O. S.; Baltrusaitis, J.; Cuadra-Rodriguez, L. A.; Collins, D. B.; Ruppel, M. J.; Bertram, T. H.; Prather, K. A.; Grassian, V. H. Inside versus Outside: Ion Redistribution in Nitric Acid Reacted Sea Spray Aerosol Particles as Determined by Single Particle Analysis. *J. Am. Chem. Soc.* **2013**, *135* (39), 14528−14531.

(20) Hughes, L. S.; Allen, J. O.; Bhave, P.; Kleeman, M. J.; Cass, G. R.; Liu, D. Y.; Fergenson, D. P.; Morrical, B. D.; Prather, K. A. Evolution of Atmospheric Particles along Trajectories Crossing the Los Angeles Basin. *Environ. Sci. Technol.* **2000**, *34* (15), 3058−3068.

(21) Bertram, T. H.; Cochran, R. E.; Grassian, V. H.; Stone, E. A. Sea Spray Aerosol Chemical Composition: Elemental and Molecular Mimics for Laboratory Studies of Heterogeneous and Multiphase Reactions. *Chem. Soc. Rev.* **2018**, *47* (7), 2374−2400.

(22) Trueblood, J. V.; Alves, M. R.; Power, D.; Santander, M. V.; Cochran, R. E.; Prather, K. A.; Grassian, V. H. Shedding Light on Photosensitized Reactions within Marine-Relevant Organic Thin Films. *ACS Earth Sp. Chem.* **2019**, *3*, 1614−1623.

(23) Sauer, J. S.; Mayer, K. J.; Lee, C.; Alves, M. R.; Amiri, S.; Bahaveolos, C.; Barnes, E. B.; Crocker, D. R.; Dinasquet, J.; Garofalo, L. A. et al. The Sea Spray Chemistry and Particle Evolution Study (SeaSCAPE): Overview and Experimental Methods. *Environ. Sci. Process. Impacts*, in press, **2021**.

(24) Angle, K. J.; Crocker, D. R.; Simpson, R. M. C.; Mayer, K. J.; Garofalo, L. A.; Moore, A. N.; Mora Garcia, S. L.; Or, V. W.; Srinivasan, S.; Farhan, M. Acidity across the Interface from the Ocean Surface to Sea Spray Aerosol. *Proc. Natl. Acad. Sci. U. S. A.* **2021**, *118* (2), 1−6.

(25) Gherman, T.; Venables, D. S.; Vaughan, S.; Orphal, J.; Ruth, A. A. Incoherent Broadband Cavity-Enhanced Absorption Spectroscopy in the near-Ultraviolet: Application to HONO and NO_2. *Environ. Sci. Technol.* **2008**, *42* (3), 890−895.

(26) Kraus, S. *DOASIS: A Framework Design for DOAS*; University of Mannheim: Mannheim, Germany, 2006.

(27) Stutz, J.; Kim, E. S.; Platt, U.; Bruno, P.; Perrino, C.; Febo, A. UV-Visible Absorption Cross Sections of Nitrous Acid. *J. Geophys. Res. Atmos.* **2000**, *105* (D11), 14585−14592.

(28) Burrows, J. P.; Dehn, A.; Deters, B.; Himmelmann, S.; Richter, A.; Voigt, S.; Orphal, J. Atmospheric Remote-Sensing Reference Data from GOME: Part 1. Temperature-Dependent Absorption Cross-Sections of NO_2 in the 231−794 Nm Range. *J. Quant. Spectrosc. Radiat. Transfer* **1998**, *60* (6), 1025−1031.

(29) Kiss, G.; Tombacz, E.; Hansson, H.-C. Surface Tension Effects of Humic-Like Substances in the Aqueous Extract of Surface Tension Effects of Humic-Like Substances in the Aqueous Extract of Tropospheric Fine Aerosol. *J. Atmos. Chem.* **2005**, *50* (3), 279−294.

(30) Reeser, D. I.; Kwamena, N. O. A.; Donaldson, D. J. Effect of Organic Coatings on Gas-Phase Nitrogen Dioxide Production from Aqueous Nitrate Photolysis. *J. Phys. Chem. C* **2013**, *117* (43), 22260−22267.

(31) Zellner, R.; Exner, M.; Herrmann, H. Absolute OH Quantum Yields in the Laser Photolysis of Nitrate, Nitrite and Dissolved H_2O_2 at 308 and 351 nm in the Temperature Range 278−353 K. *J. Atmos. Chem.* **1990**, *10* (4), 411−425.

(32) Repeta, D. J.; Quan, T. M.; Aluwihare, L. I.; Accardi, A. M. Chemical Characterization of High Molecular Weight Dissolved Organic Matter in Fresh and Marine Waters. *Geochim. Cosmochim. Acta* **2002**, *66* (6), 955−962.

(33) Carpenter, L. J.; Nightingale, P. D. Chemistry and Release of Gases from the Surface Ocean. *Chem. Rev.* **2015**, *115*, 4015.

(34) Sharpless, C. M.; Blough, N. V. The Importance of Charge-Transfer Interactions in Determining Chromophoric Dissolved Organic Matter (CDOM) Optical and Photochemical Properties. *Environ. Sci. Process. Impacts* **2014**, *16*, 654−671.

(35) von Sonntag, C.; Schuchmann, H.-P. The Elucidation of Peroxyl Radical Reactions in Aqueous Solution with the Help of Radiation-Chemical Methods. *Angew. Chem., Int. Ed. Engl.* **1991**, *30* (10), 1229−1253.

https://doi.org/10.1021/acsearthspacechem.1c00292
ACS Earth Space Chem. 2021, 5, 3056−3064

(36) Vel Leitner, N. K.; Dore, M. Hydroxyl Radical Induced Decomposition of Aliphatic Acids in Oxygenated and Deoxygenated Aqueous Solutions. *J. Photochem. Photobiol., A* **1996**, *99* (2−3), 137−143.
(37) Draper, W. M.; Crosby, D. G. Photochemical Generation of Superoxide Radical Anion in Water. *J. Agric. Food Chem.* **1983**, *31* (4), 734−737.
(38) Wang, X.; Dalton, E. Z.; Payne, Z. C.; Perrier, S.; Riva, M.; Raff, J. D.; George, C. Superoxide and Nitrous Acid Production from Nitrate Photolysis Is Enhanced by Dissolved Aliphatic Organic Matter. *Environ. Sci. Technol. Lett.* **2021**, *8* (1), 53−58.
(39) Goldstein, S.; Czapski, G.; Lind, J.; Merenyi, G. Mechanism of Decomposition of Peroxynitric Ion (O_2NOO^-): Evidence for the Formation of $O_2^{\bullet -}$ and $^{\bullet}NO_2$ Radicals. *Inorg. Chem.* **1998**, *37* (16), 3943−3947.
(40) Gupta, D.; Harish, B.; Kissner, R.; Koppenol, W. H. Peroxynitrate Is Formed Rapidly during Decomposition of Peroxynitrite at Neutral PH. *Dalt. Trans.* **2009**, *29*, 5730−5736.
(41) Ma, J.; Liu, Y.; Han, C.; Ma, Q.; Liu, C.; He, H. Review of Heterogeneous Photochemical Reactions of NO*y* on Aerosol - A Possible Daytime Source of Nitrous Acid (HONO) in the Atmosphere. *J. Environ. Sci. (Beijing, China)* **2013**, *25* (2), 326−334.
(42) George, C.; Strekowski, R. S.; Kleffmann, J.; Stemmler, K.; Ammann, M. Photoenhanced Uptake of Gaseous NO_2 on Solid Organic Compounds: A Photochemical Source of HONO? *Faraday Discuss.* **2005**, *130* (2), 195−210.
(43) Scharko, N. K.; Martin, E. T.; Losovyj, Y.; Peters, D. G.; Raff, J. D. Evidence for Quinone Redox Chemistry Mediating Daytime and Nighttime NO_2-to-HONO Conversion on Soil Surfaces. *Environ. Sci. Technol.* **2017**, *51* (17), 9633−9643.
(44) Thorn, K.; Folan, D.; MacCarthy, P. Characterization of the International Humic Substances Society Standard and Reference Fulvic and Humic Acids by Solution State Carbon-13 (^{13}C) and Hydrogen (^{1}H) Nuclear Magnetic Resonance Spectrometry. *Water-Resources Investigations Report* **1989**, *93*, 99.
(45) McKay, G.; Rosario-Ortiz, F. L. Temperature Dependence of the Photochemical Formation of Hydroxyl Radical from Dissolved Organic Matter. *Environ. Sci. Technol.* **2015**, *49* (7), 4147−4154.
(46) Cooper, W. J.; Zika, R. G.; Petasne, R. G.; Plane, J. M. C. Photochemical Formation of H_2O_2 in Natural Waters Exposed to Sunlight. *Environ. Sci. Technol.* **1988**, *22* (10), 1156−1160.
(47) Bielski, B. H. J.; Allen, A. O. Mechanism of the Disproportionation of Superoxide Radicals. *J. Phys. Chem.* **1977**, *81* (11), 1048−1050.

https://doi.org/10.1021/acsearthspacechem.1c00292
ACS Earth Space Chem. 2021, 5, 3056−3064